

Effects of Long-Range Correlations in Random-Mass Dirac Fermions

Koujin Takeda*

Institute for Cosmic Ray Research, University of Tokyo, Kashiwa, Chiba, 277-8582 Japan

Ikuo Ichinose**

Department of Electrical and Computer Engineering, Nagoya Institute of Technology, Gokiso, Showa-ku, Nagoya, 466-8555 Japan

In the previous paper, we studied the random-mass Dirac fermion in one dimension by using the transfer-matrix methods. We furthermore employed the imaginary vector potential methods for calculating the localization lengths. Especially we investigated effects of the nonlocal but short-range correlations of the random mass. In this paper, we shall study effects of the long-range correlations of the random mass especially on the delocalization transition and singular behaviours at the band center. We calculate localization lengths and density of states for various nonlocally correlated random mass. We show that there occurs a “phase transition” as the correlation length of the random Dirac mass is varied. The Thouless formula, which relates the density of states and the localization lengths, plays an important role in our investigation.

I. INTRODUCTION

In the previous papers [1,2], we studied the random-mass Dirac fermions in one dimension by using the transfer-matrix methods (TMM) and imaginary-vector potential methods (IVPM). We calculated the density of states, the typical and mean localization lengths, and the multifractal scalings as a function of the energy and correlation length of the random mass. The results are in good agreement with the available analytical calculations [3,4]. We also obtained the relation between the correlation length of the random mass and the typical localization length for the short-range correlations [2].

In this paper, we shall study effects of the long-range correlations, especially on the delocalization transition and singular behaviours at the band center. This problem is interesting for various reasons. Very recently finite mobility edges are observed in the one-dimensional Anderson model with the long-range correlated potentials though it is widely believed that (almost) all states are localized in spatial one dimension [5,6]. Similar phenomena are observed also in the aperiodic Kronig-Penney model [7]. In contrast to the above models, the system of the random-mass Dirac fermions belongs to the universality class of the *chiral* orthogonal ensemble and therefore the extended states exist at the band center though the others are localized for the white-noise random mass. Long-range correlations of the disorder may change this feature. This problem has not been addressed in detail so far. As the model is closely related with the random-bond XY model, the random Ising model, etc., the results are interesting both theoretically and experimentally.

This paper is organized as follows. The model and numerical methods are explained in the previous paper [2]. In Sec.2, we shall explain how to make a long-range correlated random Dirac mass numerically. We shall consider two types of the telegraphic random mass, i.e., in the first one magnitudes of the random mass are long-range correlated random variables (LRCRV) with fixed interval distances between kinks whereas in the second one interval distances between kinks are LRCRV with a fixed random mass magnitude. In the present study, we employ the first one in the above for it generates various correlations of the Dirac mass more easily than the second one. In Sec.3, numerical results are given. We calculate the localization lengths and the density of states (DOS) directly by using the TMM and IVPM though in most of studies of one-dimensional random models elaborated techniques like the Hamiltonian mapping, the renormalization group, etc. are used for calculating the Lyapunov exponent. For the white-noise and short-range correlated random mass, the DOS $\rho(E)$ diverges as $\rho(E) \propto \frac{1}{E^{|\log E|^3}}$ where E is the energy measured from the band center. Similarly the typical localization length $\xi(E) \propto |\log E|$. This means that there are extended states at the band center. We study how these behaviours change by the existence of the long-range correlations of the Dirac mass. We show that there is a kind of “phase transition” as the correlation length is varied. Section 4 is devoted to conclusion.

II. MODELS AND LONG-RANGE CORRELATED RANDOM MASS

Hamiltonian of the random-mass Dirac fermion is given by

$$\begin{aligned}\mathcal{H} &= \int dx \psi^\dagger h \psi, \\ h &= -i\sigma^z \partial_x + m(x)\sigma^y,\end{aligned}\tag{1}$$

where $\vec{\sigma}$ are the Pauli matrices and $m(x)$ is the telegraphic random mass. It is known that almost all energy eigenstates of the Hamiltonian (1) away from the band center are localized for short-range correlated $m(x)$ [2]. There we calculated localization length of each state by introducing an imaginary-vector potential (IVP) \tilde{g} as suggested by the work of Hatano and Nelson [8]. In an IVP, all localized states tend to extend and a ‘‘critical’’ value of IVP \tilde{g}_c at which a state becomes extended, ‘‘determines’’ its localization length at $\tilde{g} = 0$ [2].

In this paper we shall consider the long-range correlated configurations of $m(x)$ and study delocalized states by the TMM and IVP. Numerical methods which generate potentials correlated by the power law was recently invented by Izrailev *et.al.* and Herbut [6,9]. We briefly review it for we shall use it for the present studies.

Let us consider a spatial lattice and random potential $\epsilon(n)$ sitting on the sites which has correlation $\chi(n)$,

$$[\epsilon(m) \epsilon(n)]_{\text{ens}} = C \chi(|m - n|),\tag{2}$$

where n and m are site indices, and C is a constant. Here we suppose that $\chi(n)$ is given and define $\tilde{c}(k)$ from $\chi(n)$ as follows,

$$\tilde{c}(k) = \left(\tilde{\chi}(k)\right)^{1/2},\tag{3}$$

where $\tilde{\chi}(k)$ is the Fourier transformation of $\chi(n)$;

$$\tilde{\chi}(k) = \sum_{n=-\infty}^{\infty} \chi(n) e^{ikn}.\tag{4}$$

We also introduce another random site potential $r(n)$ which is distributed uniformly in the range $[-1, 1]$ with the delta-function white-noise correlation;

$$[r(m) r(n)]_{\text{ens}} \propto \delta_{mn}.\tag{5}$$

Then we can construct random potential $\epsilon(n)$ as follows by using the white-noise potential $r(m)$ and the inverse Fourier transformation of $\tilde{c}(k)$,

$$\epsilon(n) = C' \sum_{m=-\infty}^{\infty} r(m) c(m - n),\tag{6}$$

where C' is another constant. However, we cannot perform the infinite summation in (6) in the practical numerical calculation, and therefore we replace it with the finite summation as follows,

$$\epsilon(n) = C' \sum_{m=-k/2}^{k/2} r(m) c(m - n).\tag{7}$$

where k is a finite number which is much larger than the number of sites in the system. We use the periodic boundary condition for the numerical calculation in subsequent sections and set $k \simeq 10^4 + (\text{number of sites})$.

We can easily verify that the random variable $\epsilon(n)$ in (7) satisfies Eq.(2). If we choose $c(m)$ as

$$c(m) = \frac{1}{|m|^\alpha},\tag{8}$$

with some constant α , then the correlator of the random potential becomes

$$[\epsilon(m) \epsilon(n)]_{\text{ens}} \sim \frac{1}{|m - n|^{2\alpha - 1}}.\tag{9}$$

With this procedure, we can generate power-law correlated random potential. Similarly, we can generate exponentially correlated random potential if we choose the modified Bessel function K_0 as $c(m)$.

In the practical calculation, there is a subtle point in the normalization of the random potential $\epsilon(n)$ in Eq.(9) when we vary the system size L [10]. We determine the normalization of $\epsilon(m)$ (namely the value of C') in such a way that the typical value of $\epsilon(m)$ does not change. Then as a result, the strength of correlation does *not* change for various system size L if we fix $|m - n|$ in Eq.(9).

The above method generates the random potential at each site. Therefore, when we fix the distances between kinks and vary the magnitudes of $m(x)$ for generating random $m(x)$, we can directly use the above methods (see Fig.1). We can easily extend TMM to the above type of random mass $|m(x)|$. Numerical studies of this system will be reported in the following section.

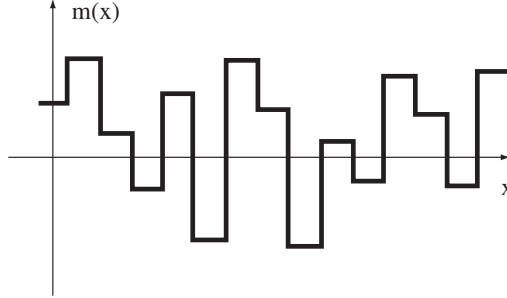


FIG. 1. An example of $m(x)$

On the other hand, we can also use the above method for generating random distances between kinks with fixed value of $|m(x)|$. This is the subject in our previous papers [1,2].

III. LONG-RANGE CORRELATED DISORDERS

We focus on the system with exponential and power-law correlated random mass in this section. Each correlation is parameterized as follows;

$$\begin{aligned} [m(x) m(y)]_{\text{ens}} &= \frac{g}{2\lambda} \exp\left(\frac{-|x-y|}{\lambda}\right), \text{ for exp-decay} \\ [m(x) m(y)]_{\text{ens}} &= \frac{C}{|x-y|^{\alpha_{pw}}}, \text{ for the power-law decay} \end{aligned} \quad (10)$$

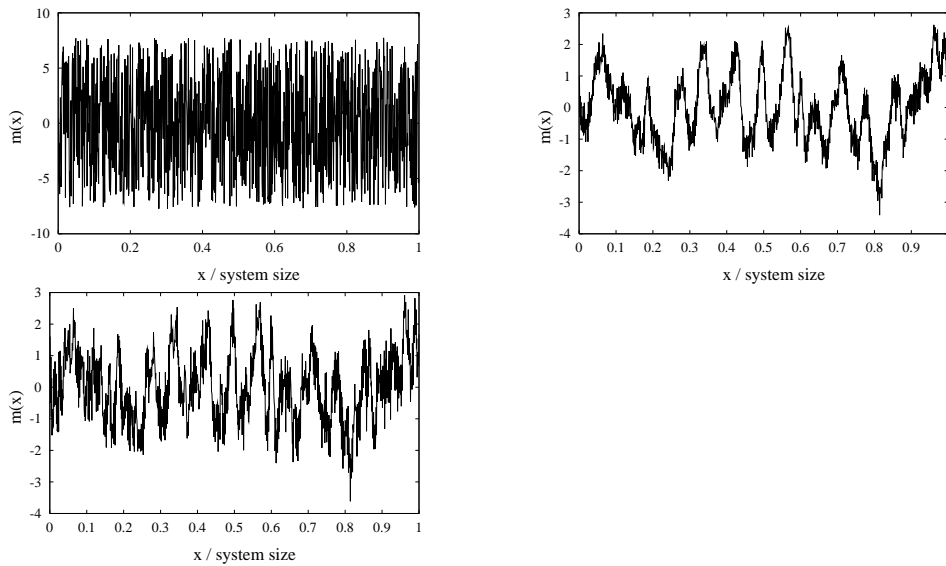


FIG. 2. An example of $m(x)$ in the case of white-noise disorder(top left), exponentially correlated(top right) and power-law correlation(bottom): We set 2000 kinks in these systems. By the numerical analysis, correlation length (per system size) λ is calculated as 0.16 in exponentially correlated case and α_{pw} is 0.68 in power-law case.

where g, λ, C and α_{pw} are constants. Dimensions of the parameters are $[\lambda] = M^{-1}$, $[g] = M^1$, $[C] = M^{2-\alpha_{pw}}$, respectively. As we explained in Sec.2, we consider the random mass of random magnitude with fixed distances between kinks. Prototype of the configuration is given in Fig.2. In this case $m(x)$ is generated rather similarly to $\epsilon(n)$ in Sec.2 though the continuum space is considered here instead of the spatial lattice. As in the previous paper [2], we use the IVPM and TMM in order to calculate the localization lengths.

We first calculate the correlation $[m(x)m(0)]_{\text{ens}}$ numerically which is expected to exhibit the exponential and power-law decay, respectively. The result is shown in Fig.3. The correlator actually shows the expected behaviour in each case, though the parameters of the correlation are slightly smaller than the analytical values, which are λ in exponential-decay case and α_{pw} in power-law decay case, respectively. We think that this is due to the finiteness of numbers of kinks and/or *finite* Fourier transformation in the scheme which we explained in the previous section. (The values of α_{pw} , λ and the parameters in Tables 1 and 2 are calculated directly from the two-point correlation function of the random mass obtained numerically.)

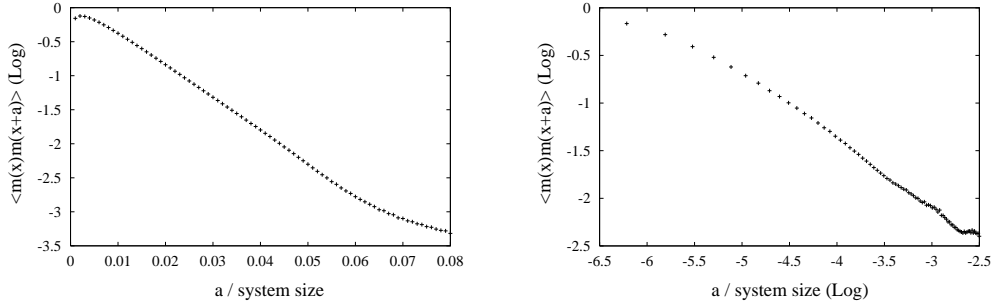


FIG. 3. Correlation of $m(x)$ in the case of exponentially correlation(left) and power-law correlation(right): Each case corresponds to random $m(x)$ shown in Fig.2. In these cases, we can consider that randomness has exponential or power-law correlation for about 10 percent of system size. We fix the parameters in Table 1 (exponential case) and 2 (power-law case) using this numerical result. (In order to fix these parameters, we used the data points in the range $0.003 < a < 0.015$ for exponential case ($0.01 < a < 0.05$ for $g\lambda = 12$) and $0.01 < a < 0.1$ for power-law case.)

Next we show the energy dependence of typical localization length in the system with the white-noise random mass. (We obtain “typical” localization length as a function of energy E by averaging localization lengths of the eigenstates within a small range of energy ΔE .) In Fig.4, we show the ratio of the numerical results to the available analytical expression which takes the form

$$\xi(E) \propto |\log(E/2g)|, \quad (11)$$

where the parameter g gives the magnitude of $m(x)$,

$$[m(x) m(y)]_{\text{ens}} = g \delta(x - y). \quad (12)$$

It is easily seen that the limit $\lambda \rightarrow 0$ in Eq.(10) corresponds to Eq.(12). As Fig.4 shows, our numerical calculations and the analytical expression (11) are in good agreement. This guarantees validity of our methods of calculation, the TMM and IVPM.

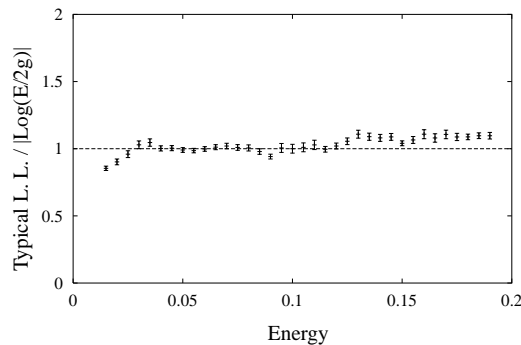


FIG. 4. The energy dependence of localization length in the case of white-noise disorder : We set $L(\text{system size})=50, 1000$ kinks in the system and $g = 1$. Ratio is normalized at $E = 0.10$ and data are averaged within small energy slice ΔE , We set $\Delta E = 0.02$ here.

We calculated the energy dependences of the localization length in the case of exponentially correlated disorder in Eq.(10). In Fig.5, we show the ratio of numerical calculations to the analytical expression of the white-noise case $|\log(E/2g)|$. We vary the correlation length λ of $m(x)$. The ratio is almost constant for small $g\lambda$. However as $g\lambda$ is getting large, the numerical results obviously deviate from $|\log(E/2g)|$.

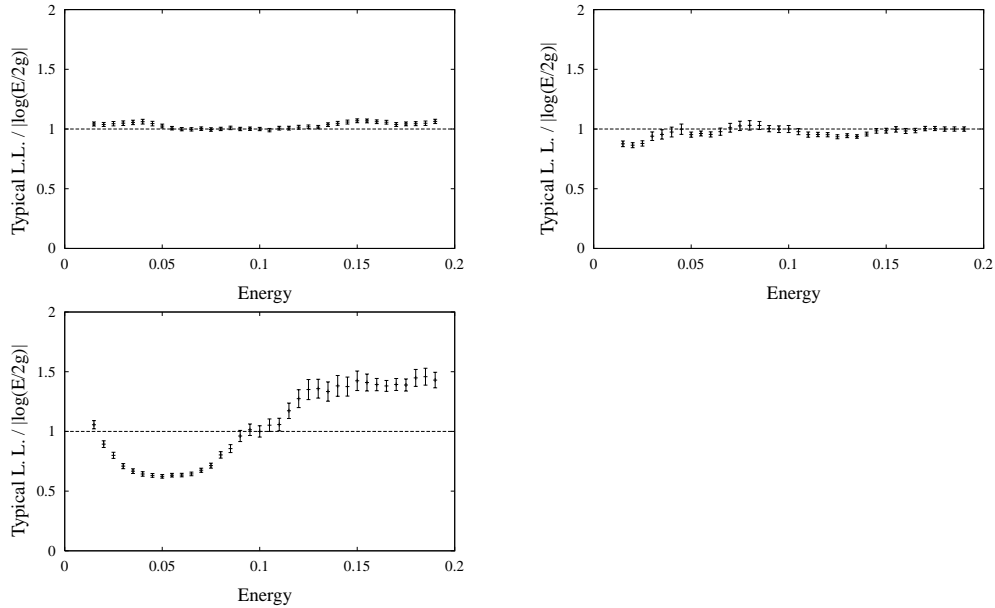


FIG. 5. The energy dependence of localization length in the case of exponentially correlated random mass: We set $L(\text{system size}) = 50$ and 1000 kinks in the system. The ratios are normalized at $E = 0.1$ and data are averaged within energy slice $\Delta E = 0.02$. Values of λ and g are given in Table 1. The ratio is almost constant for small $g\lambda$, but it deviates from constant in the case of large $g\lambda$.

Table 1. Parameters of exponential correlation.

	λ	g	$g\lambda$
top left	0.28	2.9	0.80
top right	1.2	2.4	2.8
bottom	8.1	1.5	12

We show the energy dependence of the localization length in the case $g\lambda = 12$ in Figs.5 (bottom) and 6. We can conclude that the localization length diverges only at $E = 0$ even for very large $g\lambda$. This means that exponential correlation of the random mass gives no significant effect on the *Anderson transition*. Actually this result can be expected from the study in the previous paper [2].

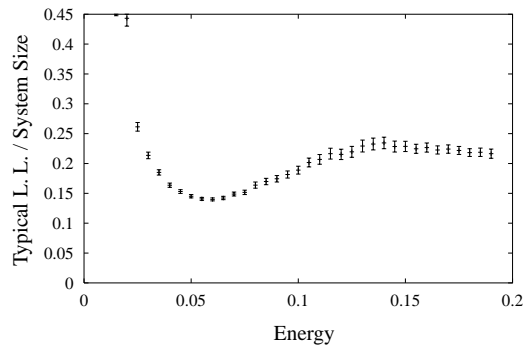


FIG. 6. The energy dependence of localization length in the case of exponentially correlated random mass (especially the case of large $g\lambda$): This data corresponds to the one at the bottom in Fig.5. Data are averaged within energy slice $\Delta E = 0.02$. Divergence of localization length is found only at the point $E = 0$.

However the result also shows that singular behaviour of the localization length at $E = 0$ for the exponentially correlated $m(x)$ (with large $g\lambda$) may be *different from* that of the white-noise case. From the analytical study by using supersymmetry [4], the localization length is obtained in powers of $g\lambda$ and more dominant terms like $|\log(E/2g)|^2$ etc. appear in higher-order terms of $g\lambda$.

We therefore investigate the behaviour of the localization length near the band center $E = 0$ rather in detail. In Fig.7 we show the ratio of the numerically obtained localization length to $|\log(E/2g)|^\delta$, where δ takes the value 1,2,3 and 4. In some energy regions, the energy dependence is fitted better by the power $\delta = 2$ or 3 than $\delta = 1$.

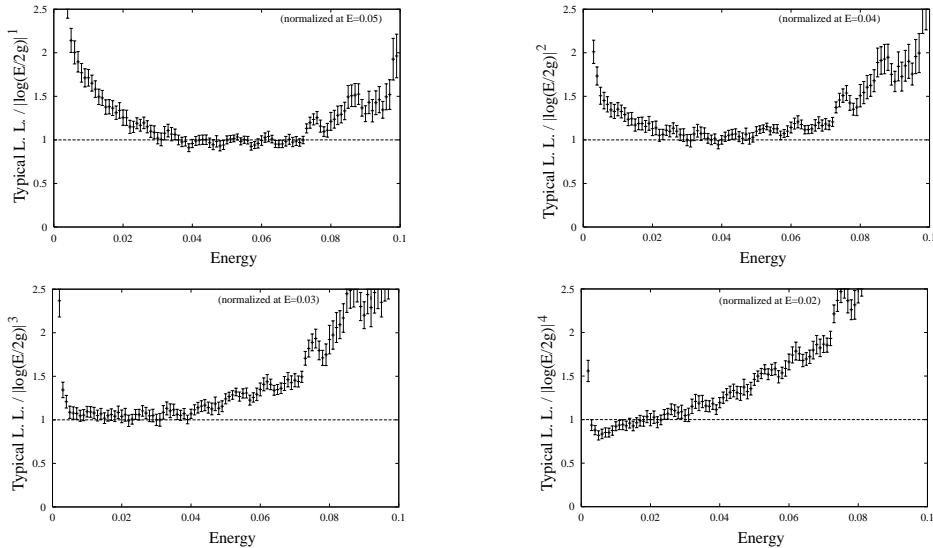


FIG. 7. Ratio of the Localization length to $|\log(E/2g)|^\delta$: Here we set $L(\text{system size}) = 50$, and δ takes the value 1,2,3 and 4. Data are averaged within energy slice $\Delta E = 0.01$.

We can expect the above result by the analytical study. In the previous paper, [4] the DOS $\rho(E)$ is obtained analytically as follows for the exponentially correlated random mass;

$$\rho(E) = \frac{A_1}{\frac{E}{2g}|\log(E/2g)|^3} + \frac{A_2}{\frac{E}{2g}|\log(E/2g)|^4} + \frac{A_3}{\frac{E}{2g}|\log(E/2g)|^5}, \quad (13)$$

where A_i ($i = 1, 2, 3$) are polynomials of $g\lambda$,

$$\begin{aligned} A_1 &= \frac{1}{2} - \frac{26}{15}(g\lambda)^2 - \frac{4}{105}(g\lambda)^3 + \dots, \\ A_2 &= -3(g\lambda) - 2(g\lambda)^2 + \dots, \\ A_3 &= 4(g\lambda)^2 + \dots. \end{aligned} \quad (14)$$

In order to verify Eq.(13), we calculate the DOS numerically for relatively small $g\lambda (< 1)$ and compare the result with Eq.(13). From Fig.8, it is obvious that $\rho(E)$ up to the third-order term of $(g\lambda)$ is in better agreement with the numerical result than the first-order one.

Using Thouless formula for 1D random hopping tight binding model [11] (whose low-energy field theory is the random-mass Dirac fermion),

$$\frac{1}{\xi(E)} \propto \int_0^{|E|} \log\left(\frac{E}{E'}\right) \rho(E') dE', \quad (15)$$

we can show that corresponding to the second and the third term in (13) there are contributions to the localization length like $|\log(E/2g)|^2$ and $|\log(E/2g)|^3$ if these terms become dominant in the DOS. It is also expected that the ratio is not constant for any range of energy in the case $\delta = 4$, because DOS has no term proportional to $1/E|\log(E/2g)|^6$.

These numerical results and the above discussion indicate that the nonlocal correlations of the random mass generate nontrivial effect on the localization. One may expect that for large $g\lambda$ the perturbative calculation in powers of $g\lambda$

breaks down for the DOS and the localization length and $\rho(E)$ and $\xi(E)$ exhibit different singular behaviours at $E = 0$. Especially the terms like $|\log E|^\delta$ in $\xi(E)$ may be summed up and the localization length may behave as

$$\xi(E) \sim E^{-\beta} \quad (16)$$

for large $g\lambda$ where β is a constant. In Fig.9 we show the log-log plot of $\xi(E)$ v.s. energy. The numerical data are obviously on a straight line and therefore the singular behaviour (16) is verified.

From the Thouless formula (15), we also expect the power behaviour of the DOS. Actually it is not so difficult to show that for the DOS parameterized as

$$\rho(E) \sim E^{-\eta} |\log E|^{-\gamma}, \quad (17)$$

where η and γ are parameters, the Thouless formula (15) gives the following localization length,

$$\begin{aligned} \xi(E) &\sim E^{-1+\eta} |\log E|^{-1+\gamma}, \quad \text{for } \eta \neq 1, \\ \xi(E) &\sim |\log E|^{-2+\gamma}, \quad \text{for } \eta = 1. \end{aligned} \quad (18)$$

In Fig.10 we show the calculations of the DOS for $g\lambda = 12$. It is obvious that the DOS $\rho(E)$ behaves as

$$\rho(E) \sim E^{-\beta'}. \quad (19)$$

We cannot fix the exponent γ in Eqs. (17) and (18) from these numerical calculations. However, we can conclude that $\eta \neq 1$ in the case $g\lambda = 12$. This confirms the power-law behaviour of the localization length near the band center $E = 0$, which differs from the behaviour of the white-noise disorder case.

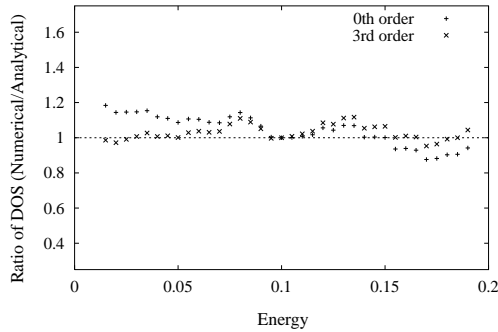


FIG. 8. The energy dependence of DOS in the case of exponentially correlated random mass (especially the case of large $g\lambda$): We show the ratio of DOS we calculated numerically to the one obtained analytically. Ratio is normalized at $E = 0.10$ and data are averaged within energy slice $\Delta E = 0.02$. We set $g\lambda = 0.80$ here. (This corresponds to the case of the top left figure in Fig.5.) In order to show the effect of exponential correlation, we use DOS obtained analytically up to 0th and 3rd order of $g\lambda$ expansion, respectively.

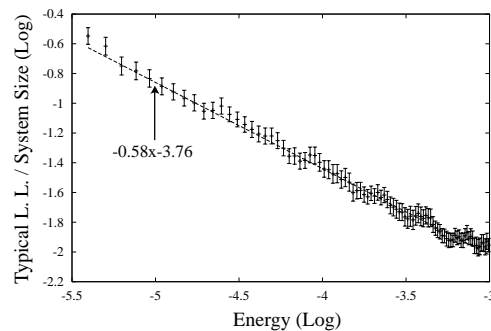


FIG. 9. The energy dependence of localization length in the case of exponentially correlated random mass (especially the case of large $g\lambda$): Data are averaged within energy slice $\Delta E = 0.005$. We set $g\lambda = 12$ here. (This corresponds to the case of the bottom figure in Fig.5.) χ^2 (per freedom) value of this fitting is 0.36.

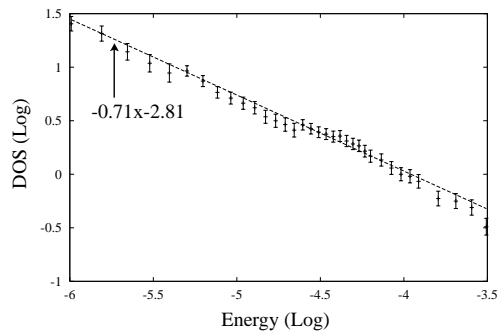


FIG. 10. The energy dependence of DOS in the case of exponentially correlated random mass (especially the case of large $g\lambda$): Data are averaged within energy slice $\Delta E = 0.005$. We set $g\lambda = 12$ here. (This corresponds to the case of the bottom figure in Fig.5.) We set energy slice $\Delta E = 0.002, 0.006$ and 0.01 for $E < 0.005, 0.005 < E < 0.01$ and $0.01 < E$ respectively. The interval of data points are $5 \times 10^{-4}, 1 \times 10^{-3}$ and 2.5×10^{-3} for $E < 0.015, 0.015 < E < 0.02$ and $0.02 < E$ respectively. DOS is normalized at log $E = -4.0$. χ^2 value of this fitting is 0.64.

Let us turn to the study on the power-law correlated random mass in Eq.(10);

$$[m(x) m(y)]_{\text{ens}} = \frac{C}{|x - y|^{\alpha_{pw}}}.$$

Here we emphasize significance of the power-law correlation of the randomness to the Anderson transition etc. This is due to the scale-free property of the power-law correlation, and this type of correlations may not be negligible even though system size is very large.

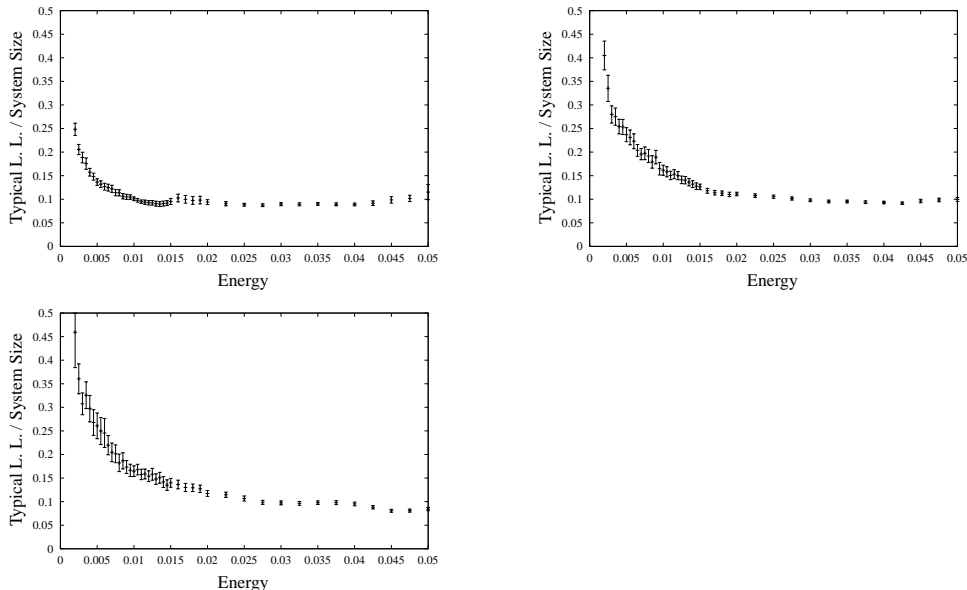


FIG. 11. The energy dependence of localization length in the case of power-law correlated random mass: We set $L(\text{system size}) = 50$ and 1000 kinks in the system. α_{pw} 's and C 's in Eq.(10) are given in Table 2. Localization length is averaged within energy slice $\Delta E = 0.003, 0.004, 0.006$ and 0.01 for $0 < E < 0.01, 0.01 < E < 0.015, 0.015 < E < 0.02$ and $0.02 < E$ respectively. The interval of data points are $5 \times 10^{-4}, 1 \times 10^{-3}$ and 2.5×10^{-3} for $E < 0.015, 0.015 < E < 0.02$ and $0.02 < E$ respectively. Divergences of localization length are observed only at $E = 0$.

	α_{pw}	C
top left	0.68	0.016
top right	0.34	0.056
bottom	0.099	3.1

Table 2. Parameters of power-law correlation.

In Fig.11, we show the energy dependences of the localization length in the system with power-law correlated random mass. We choose value of the parameter α_{pw} as in Table 2. These results show that localization length diverges only at $E = 0$, as in the case of white-noise and exponentially correlated disorder. This behaviour does not depend on the value of α_{pw} .

We also study the system size dependence of the localization length. Results are shown in Fig.12. We conclude that extended states exist only at the band center $E = 0$.

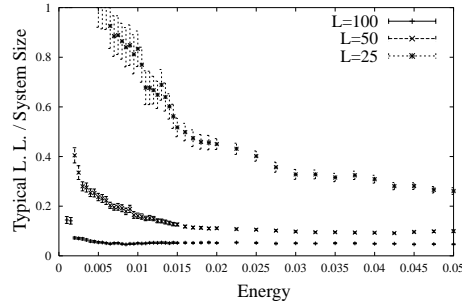


FIG. 12. The system size dependence of typical localization length in the case of power-law correlation: Parameters except for the system size and number of kinks are the same used in the top right figure in Fig.11. (Here we fix the number of kinks per system size.) Divergence of localization length is observed at $E = 0$ in each case.

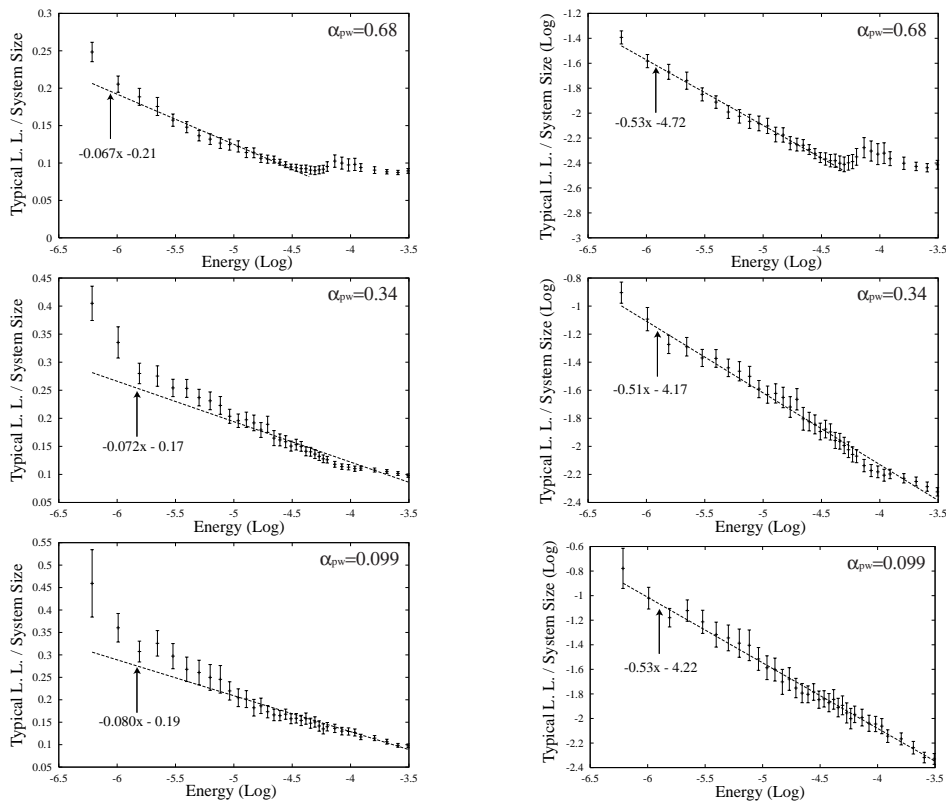


FIG. 13. Log-uni and log-log plot of the data shown in Fig.9: The left column is log-uni and the right one is log-log plot.

α_{pw}	incline (log-log)	χ^2 /freedom (log-log)	(log-uni)
0.68	-0.53	0.25	1.08
0.34	-0.51	0.83	3.05
0.099	-0.53	0.22	1.10

Table 3. Results of linear fit to log-uni and log-log plot: We use the data in the range $-6 < \log E < -3.5$ ($-6 < \log E < -4.4$ for $\alpha_{pw} = 0.68$). The incline in the table corresponds to $-\beta$ in Eq.(16). χ^2 values for log-log plot are estimated smaller than log-uni plot.

In order to investigate the singular behaviours of the Dirac fermions with the long-range correlated random mass, we change the linear scale of energy and localization length in Fig.11 to log-uni and log-log scale plots in Fig.13.

If the data in the log-uni scale are on a straight line, the energy dependence of localization length $\xi(E)$ is given by

$$\xi(E) \propto |\log E| + \text{const.} \quad (E \rightarrow 0), \quad (20)$$

as in the white-noise case. On the other side, if the data in the log-log scale are on a straight line, the energy dependence of $\xi(E)$ is given as Eq.(16) $\xi(E) \propto E^{-\beta}$ up to possible $|\log E|$ corrections. From Fig.13 and Table 3, we can conclude that E -dependence of $\xi(E)$ is given by Eq.(16). The exponent β is estimated as in Table 3.

The above singular behaviour in the present system at $E = 0$, i.e., Eq.(16) is also confirmed by the calculation of the DOS near the band center $E = 0$. We show the energy dependence of the DOS in Fig.14.

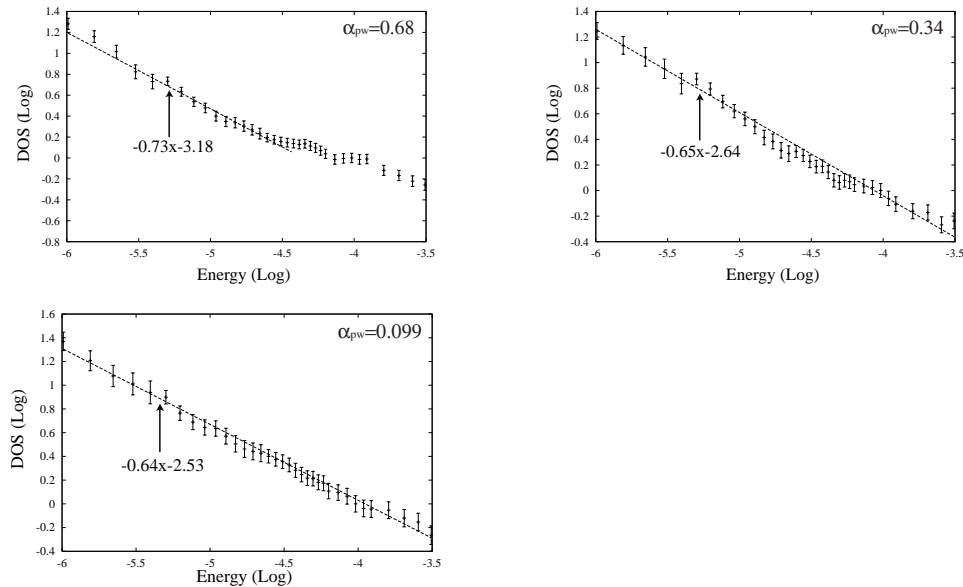


FIG. 14. The energy dependence of DOS in the case of power-law correlated random mass: DOS is calculated as the number of states within energy slice $\Delta E = 0.002, 0.006$ and 0.01 for $E < 0.005, 0.005 < E < 0.01$ and $0.01 < E$ respectively. The interval of data points are $5 \times 10^{-4}, 1 \times 10^{-3}$ and 2.5×10^{-3} for $E < 0.015, 0.015 < E < 0.02$ and $0.02 < E$ respectively. DOS are normalized at $\log E = -4.0$.

α_{pw}	incline	$\chi^2/\text{freedom}$
0.68	-0.73	0.86
0.34	-0.65	0.97
0.099	-0.64	0.25

Table 4. Results of linear fit to DOS log-log plot: We use the data in the range $-6 < \log E < -3.5$ ($-6 < \log E < -4.4$ for $\alpha_{pw} = 0.68$). The incline in the table corresponds to $-\beta'$ in Eq.(21).

The result indicates that the DOS $\rho(E)$ diverges as

$$\rho(E) \propto E^{-\beta'} \quad (E \rightarrow 0), \quad (21)$$

with the constant β' given in Table 4. From the Thouless formula Eq.(15), β in Eq.(16) and β' in Eq.(21) must satisfy the relation like

$$\beta + \beta' = 1. \quad (22)$$

From Tables 3 and 4, it is seen that $\beta + \beta'$ is almost unity as it is expected. In order to determine the exponent γ of the possible $|\log E|$ correction in Eqs.(17) and (18), calculation of the localization and the DOS for wider range of E is required.

In the above we concluded that the power-law correlation of the random mass in Eq.(10) does not influence the phase structure of the system and extended states appear only at $E = 0$. This result may seem to be in contradiction to the results obtained in the previous papers [5–7], in which nonlocally-correlated Anderson, random hopping and random Kronig-Penney (random delta potential) models are studied and in each model the presence of a *nontrivial mobility edge* is observed at a finite energy. However, the correlations of randomness in their models are different from those of the present study. Actually in one of these papers [5], the following correlation was used for the one-dimensional random hopping tight binding(RHTB) model,

$$[(\epsilon_i - \epsilon_j)^2]_{ens} \propto |i - j|^{\omega-1}, \quad (23)$$

where ω is a non-negative constant and they concluded that a delocalized phase appears in a finite region around $E = 0$ in the case of $\omega = 1.5$. As the random-mass Dirac fermion is a low-energy effective field theory of the RHTB model, the above result is relevant to the present study. As in the present study we consider the case $\omega < 1$, their results are *consistent* with ours.

We use the random variables in Eq.(23) for $m(x)$ in the present field-theory model and calculate the localization length as before. The result of the numerical study is shown in Fig.15. From these calculations, we cannot find any *finite region* of extended states around $E = 0$ even in the case $\omega = 1.5$. However, the system size may not be large enough for this calculation.

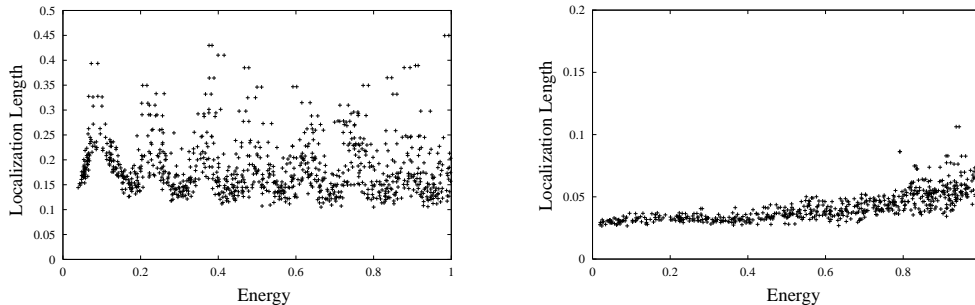


FIG. 15. Localization length and energy of the eigenstates in correlated disorder system: Correlation of $m(x)$ is given in Eq.(23). We set $L(\text{system size})=50$ and 200 kinks in the system. We set $\omega = 0$ at the left and $\omega = 1.5$ at the right.

IV. CONCLUSION

In this paper, we studied the Dirac fermion with the long-range correlated random mass by using the TMM and IVP. We are especially interested in the delocalization transition or the existence of a finite mobility edge. Recent studies on the Anderson model, random hopping model and random Kronig-Penney model indicate the existence of finite mobility edges. However we found that extended states exist only at the band center $E = 0$ as in the white-noise random variable case.

We also studied the localization length as a function of E rather in detail. We found that in the case of short-range correlation $\xi(E) \propto |\log E|$ for small E whereas $\xi(E) \propto E^{-\beta}$ ($\beta \sim 0.5$) for the long-range correlation of the random mass. The above conclusion is supported by the calculation of the DOS through the Thouless formula. We hope that the above behaviour of the localization length is observed by experiment of the random spin model because the localization length is directly related with the spin-spin correlation length there.

We can also calculate the multi-fractal scaling indices directly from wave functions of the random-mass Dirac fermions. Values of the indices may depend on the decay power of the correlation of the random mass. Results will be reported in a future publication [12].

* Electronic address: takeda@icrr.u-tokyo.ac.jp

** Electronic address: ikuo@ks.kyy.nitech.ac.jp

- [1] K. Takeda, T. Tsurumaru, I. Ichinose, and M. Kimura, Nucl. Phys. B **556** (1999) 545.
- [2] K. Takeda and I. Ichinose, J. Phys. Soc. Japan **70** (2001) 3623.
- [3] L. Balents and M. P. A. Fisher, Phys. Rev. B **56** (1997) 12970.
- [4] I. Ichinose and M. Kimura, Nucl. Phys. B **554** (1999) 607; *ibid*, B **554** (1999) 627.
- [5] F. A. B. F. de Moura and M. L. Lyra, Phys. Rev. Lett. **81** (1998) 3735; Physica A **266** (1999) 465.
- [6] F. M. Izrailev and A. A. Krokhin, Phys. Rev. Lett. **82** (1999) 4062.
- [7] F. M. Izrailev, A. A. Krokhin and S. E. Ulloa, Phys. Rev. B **63** (2001) 041102.
- [8] N. Hatano and D. R. Nelson, Phys. Rev. Lett. **77** (1996) 570; Phys. Rev. B **56** (1997) 8651.
- [9] I. F. Herbut, cond-mat/0007266.
- [10] J. W. Kantelhardt et. al. Phys. Rev. Lett. **84** (2000) 198; F. A. B. F. de Moura and M. L. Lyra, Phys. Rev. Lett. **84** (2000) 199.
- [11] D. J. Thouless, J. Phys. C **5** (1972) 77; G. Theodorou and M. H. Cohen, Phys. Rev. B **13** (1976) 4597.
- [12] K. Takeda and I. Ichinose, work in progress.